Phosphor-free InGaN Nanopillar White LEDs by Random Clustering of Mono-Sized Nanospheres

Wai Yuen Fu[1] and Hoi Wai Choi[1, a)]
Department of Electrical and Electronic Engineering, the University of Hong Kong, Pokfulam Road, Hong Kong.

(Dated: 29 April 2021)

Nanosphere lithography with mono-sized nanospheres has been employed as a patterning tool of nanostructuring to achieve phosphor-free white-light emission in this study. Nanostructuring of InGaN/GaN quantum wells induces spectral blue-shift due to strain relaxation, the extent of which depends on the sizes of the nanopillars. Nano-clusters of various sizes are formed as a result of random clustering of the mono-sized nanospheres, so that the clusters emit at different wavelengths as they are strain-relaxed to different levels. A Monte Carlo simulation has been employed to simulate the clustering patterns, while molecular dynamics and $\mathbf{k}\cdot\mathbf{p}$ Schrödinger calculations have been carried out to identify the appropriate nano-cluster distribution for phosphor-free white-light emission. The fabricated device achieves a CRI of about 76 with overall luminous efficacy of 2.6 lm/W under DC operation and 11.0 lm/W under pulsed operation.

InGaN-based light-emitting diodes (LEDs) are widely used for lighting due to their high energy efficiencies and long lifetimes. LED lamps typically emit white light by combining blue light from InGaN LEDs with yellow light from a color-converting material such as phosphor. While lamps using such color conversion approaches are already more energy efficient than incandescent and gas-discharge light bulbs, unavoidable conversion losses as well as degradation of the color-converting material lowers the overall efficiencies and lifetimes of the lamps. Lamps not requiring color-converting materials, or phosphor-free white-light LEDs, would be an feasible solution for alleviating such problems[1].

There have been numerous reports on different approaches towards attaining phosphor-free polychromatic emission, including the stacking of multi-quantum wells (MQWs) of different emission wavelengths[2–4], incorporating a second set of MQWs for color conversion[5], the growth of quantum dots[6], nanowires and nanopillars[7] as well as the top-down fabrication of nanopillars[8]. The bottom-up growth approaches typically involve adjusting the properties of the MQWs, especially on the Indium content, to enable multi-wavelength emission. Nevertheless, the internal quantum efficiency (IQE) of such structures may be compromised when compared to conventional LED structures. On the other hand, devices adopting the top-down fabrication approach benefit from the higher IQEs of optimized conventional LED structures as well as enhanced light extraction efficiencies, albeit with potential plasma-induced damages to the etched sidewalls that can be minimized by wet etching[9]. Phosphor-free polychromatic light emission using top-down fabricated nanopillars is based on strain relaxation of the MQWs consequential of nanostructuring, which in turn spectral-shifts the emission towards shorter wavelengths of emission (blue-shift) due to a reduction in the Quantum Confined Stark Effect (QCSE)[10,11]. To achieve multi-wavelength emission, nanopillars of different dimensions have to be fabricated monolithically on the same chip to induce strain relaxation to different extents[12], which can be accomplished conveniently by nanosphere lithography especially for rapid prototyping[8]. For white-light emission, challenges involving fine adjustments of nanopillar dimensions in the correct ratios need to be overcome. Such nanopillars can also be patterned by electron beam lithography[13] with high precision, albeit with lower throughput and cost-effectiveness. In view of such considerations, a mono-sized nanosphere approach is proposed to realize a phosphor-free white-light LED comprising nanopillars of multiple dimensions making use of the random clustering effect. The mono-sized nanosphere patterning process has been designed with the aid of molecular dynamics simulations and Monte Carlo simulations. The nanosphere coating recipe is developed based on the simulated parameters, and a nanopillar LED has been fabricated. The optical and electrical properties of the fabricated device is comprehensively characterized.

In order to optimize the design of the nanopillar array, the relationship between nanopillar diameter, strain relaxation and spectral shift needs to be clarified. 2D molecular dynamics simulations of nanopillars with diameters ranging from 10 nm to 200 nm are performed by LAMMPS following the approach taken in our previous studies on the strain relaxation mechanisms of micropillars[14] and the design of strain-inducing nanopillars for spectral red-shifting[15]. The active region is implemented with 9 pairs of InGaN/GaN MQWs with thicknesses of ~3.6 nm (7 atomic layers) for the InGaN wells with 25% Indium content and ~13 nm (25 atomic layers) for the GaN barriers, in accordance with the parameters of the wafer used to fabricate the device, as estimated from the cross-sectional TEM images and EDX data. Fig. 1(a) plots the simulated percentages of strain relaxation averaged across all positions inside the quantum wells for the nanopillars of different diameters. The strain relaxation is calculated utilizing the mappings of in-plane strain, i.e., the strain field perpendicular to the growth direction [0002], as illustrated in Fig. 1(b). Using these values of strain relaxation, the spectral shifts can be estimated using $\mathbf{k}\cdot\mathbf{p}$ Schrödinger calculations[14,15].

As shown in Fig. 1(a), it is apparent that the strain relaxation and thus the spectral blue-shift increases exponentially

a)Electronic mail: hwchoi@hku.hk.

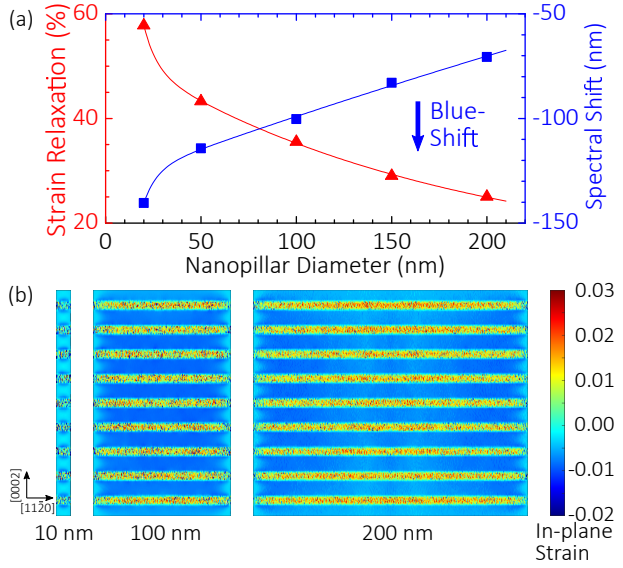

FIG. 1. (a) Simulated average strain relaxation in MQWs and corresponding spectral shift, and (b) simulated in-plane strain fields of the MQW region in nanopillars with diameters of 10 nm, 100 nm and 200 nm.

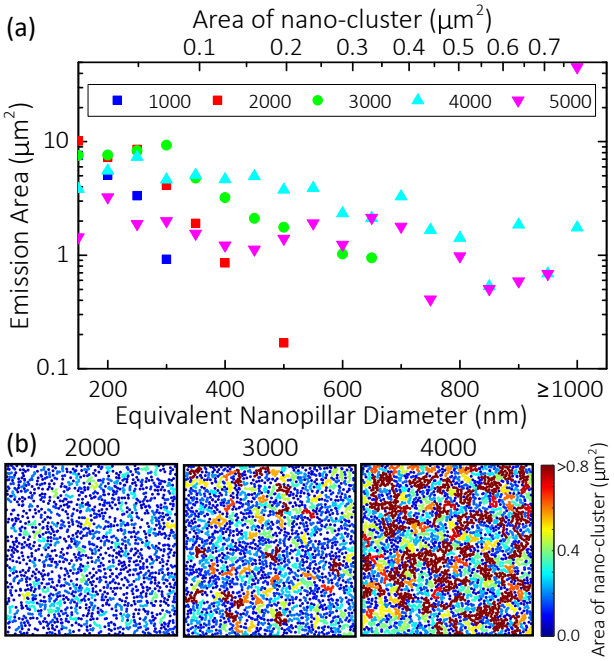

FIG. 2. (a) Results of Monte Carlo simulation of nanosphere clustering, and (b) the corresponding examples of randomly-distributed nanosphere clusters generated within a 10 μm × 10 μm region, as denoted by the black boxes.

as the nanopillar diameter decreases. The strain relaxation increases significantly as the diameter drops below 50 nm, as the strain is most relaxed within a 20 nm region near the sidewalls, as illustrated in Fig. 1(b), similar to our observations of relative spectral shift effect in our previous studies[14]. Given that the PL emission wavelength of the as-grown wafer is 600 nm, the nanopillar should be at most 50 nm in diameter so that the 43% strain relaxation can cause a spectral blue-shift of around 114 nm, hence emitting at a wavelength of 486 nm. For green light emission, a nanopillar with a diameter of 200 nm emitting at 529 nm would suffice.

While both green and blue light emissions can be achieved with nanopillars over a relatively small range of sizes, red light emission would require active regions of larger dimensions (> 1 μm^2) in order to retain the high levels of strain in MQWs. The natural clustering effect of nanosphere lithography, which is usually flagged as a disadvantage for other purposes requiring highly-ordered nanostructures such as photonic crystals, can actually be exploited to form nanostructures of non-uniform sizes using only mono-sized nanospheres. A Monte Carlo simulation has been conducted to simulate the distribution of nano-clusters formed by dispersing different amounts of nanospheres to emulate the effect of varying nanosphere concentrations in the nanosphere lithography process. In the simulation, different numbers of 150 nm-diameter nanospheres, ranging from 1000 to 5000, are dispersed across a 10 μm × 10 μm × 500 nm region without overlapping , with each case being repeated 50 times. The 2D projection of the nanospheres, which essentially is the pattern formed after etching as illustrated in Fig. 2(b), is measured and statistically plotted, as shown in Fig. 2(a).

Fig. 2(a) shows the average distribution of nano-clusters as estimated by the Monte Carlo simulations. The x-axis represents the sizes of nano-clusters formed, which is represented by either the area $A_{\text{nano-cluster}}$, or the "equivalent nanopillar diameter" $D_{\text{nanopillar}} = 2\sqrt{A_{\text{nano-cluster}}/\pi}$ for referencing to the data of Fig. 1(a). The y-axis corresponds to the summed emission area, which is the summation of the areas of all nano-clusters of that particular dimension as specified on the x-axis. As can be seen, clustering rarely occurs when the concentration is low (1000 nanospheres/ 100 μm^2). At higher concentrations, clustering occurs with cluster areas ranging from 0.018 μm^2 to 0.785 μm^2, or 150 nm to 1000 nm of "equivalent nanopillar diameter". Above concentrations of 5000 nanospheres/ 100 μm^2, the entire area is covered in one big cluster (not shown in graph). To achieve white-light emission, the size distribution of the nanosphere clusters should cover a wide range of "equivalent nanopillar diameter", corresponding to 3000 – 5000 nanospheres/ 100 μm^2 according to Fig. 2(a). Given that 20 μL of nanosphere solution is dispersed onto a 15 mm × 15 mm sample during device fabrication, the corresponding nanosphere concentration required would be about 1.6 – 2.6 mg/cm^3. Note that nanospheres with diameters of 150 nm are used both in the experiments and in the Monte Carlo simulation as silica nanospheres with diameters of less than 150 nm do not provide sufficient etch selectivity for etching through the MQWs. To further shrink the nanopillars for blue-light emission, additional wet etching is required.

The nanostructures are top-down fabricated on a metal-organic vapour-phase epitaxy (MOVPE) grown wafer on a c-plane patterned sapphire substrate. The structure consists of a 5 μm-thick undoped-GaN buffer layer, a 1.7 μm-thick n-GaN layer, 9 pairs of InGaN/GaN quantum wells, a 70 nm-thick

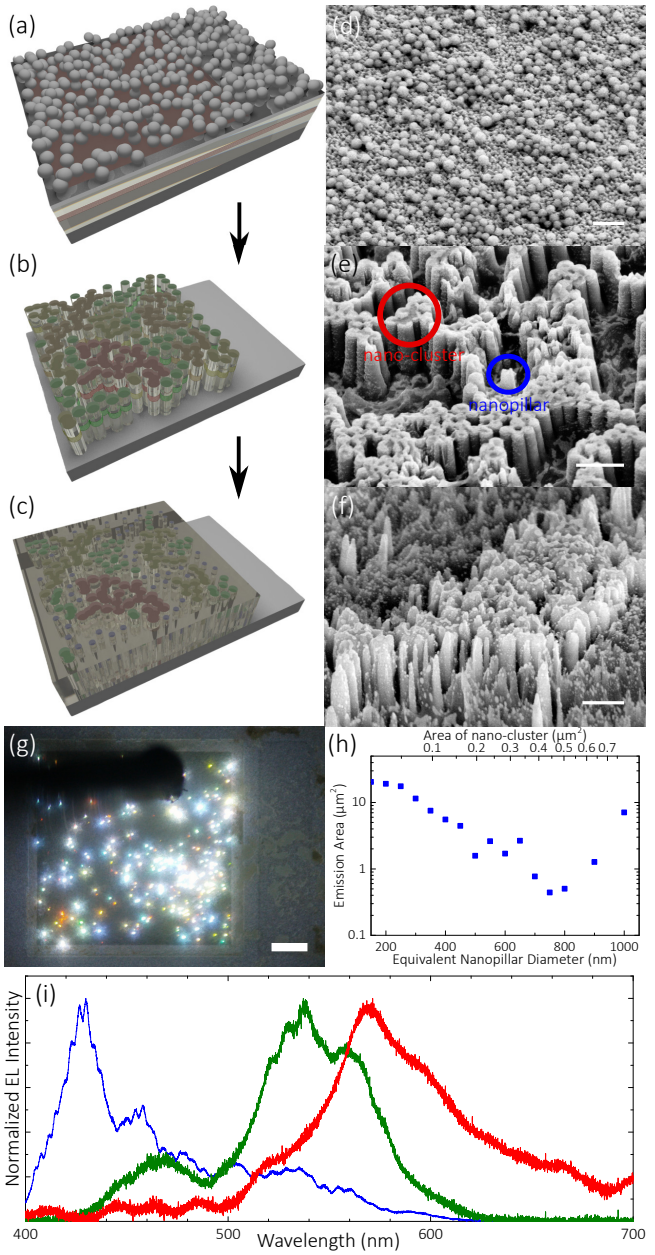

FIG. 3. Schematic diagrams depicting the fabrication process flow of the nanopillar LED, comprising of (a) coating of nano-clusters with mono-sized nanospheres, (b) ICP etching using the nano-clusters as mask, and (c) wet etch, oxide passivation and planarization by SOG with subsequent etch-back. (d), (e) and (f) show the corresponding SEM images of (a), (b) and (c), respectively. The scale bars in the SEM images are 500 nm. (g) A CCD image showing the fabricated device under operation (scale bar is 50 μm long). (h) shows the statistical size distributions of nanopillars as extracted from the SEM images. (i) shows μ-EL spectra collected from different locations across the emission region.

p-GaN spacer, an AlGaN/GaN electron blocking layer (EBL) and capped with a 330 nm-thick p-GaN layer. A 190 nm-thick ITO current spreading layer is deposited over the p-GaN layer. The fabrication process flow is illustrated in Fig. 3(a)-(c).

A 75 nm-thick Ni mask is first deposited onto the wafer to define the 250 μm by 250 μm emissive regions of the LEDs. Silica nanospheres with diameters of 150 nm are then spin-coated onto the sample, followed by inductively coupled plasma (ICP) etching for pattern transfer to form nanopillars and nano-islands within the emissive regions. The sample is then dipped into a 95°C AZ400K solution for wet etching, so that the smallest-sized 150nm nanopillars are further shrank to ~50nm for blue-light emission. Subsequently, the nanostructures are passivated by deposition of SiO_2 by plasma-enhanced chemical vapor deposition (PECVD). Spin-on-glass (SOG) is spin-coated onto the sample followed by reactive ion etching (RIE) for planarization. Finally, a current spreading layer of Ni/Au (5nm/5nm) is deposited over the planarized nanostructures, followed by deposition of Ti/Al/Ti/Au (30nm/100nm/30nm/30nm) as contact pads.

Fig. 3(d)-(f) show scanning electron microscope (SEM) images of the fabricated nanostructures at different stages of fabrication. As shown in Fig. 3(d), the nanosphere coating pattern is similar to that predicted by Monte Carlo simulation shown in Fig. 2(b), with a bit more clustering due to the natural close-packing effect of the nanospheres. Fig. 3(e) shows the nanopillars formed after ICP etching through the nanosphere pattern, comprising of both individual nanopillars as well as nano-islands due to nanospheres clustering. The size distribution of the nanopillar/ nano-clusters, as extracted from SEM images of the sample surface before wet etching, is shown in Fig. 3(h), for comparison with the simulated data in Fig. 2. The resulting active region is estimated from the SEM image to be 32.4% of the original emissive region.

Optical measurements are conducted using a radiometrically calibrated system, comprising a 4 inch-diameter Labsphere integrating sphere that is optically coupled to a spectrometer (Ocean Optics USB4000) through an optical fibre. Fig. 4 shows typical emission spectral characteristics of the phosphor-free nanopillar LED, together with that of an as-grown LED, driven at 3V to 4.5V. The electroluminescent (EL) spectrum of the nanopillar LED appears similar to that of a conventional phosphor-coated LED, with two major emission bands: a blue peak centered at around 454 nm – 468 nm , and a green/yellow peak centred at around 545 nm – 569 nm,

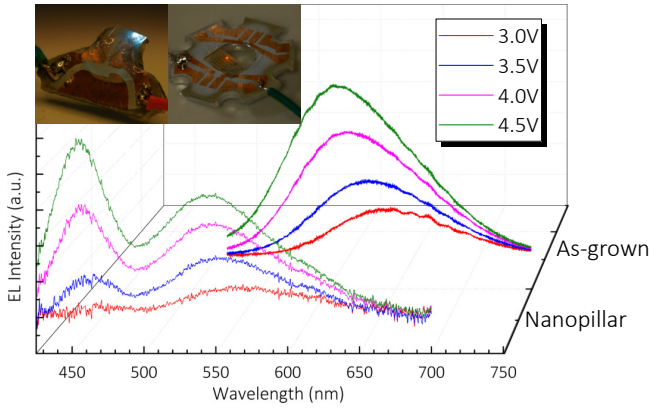

FIG. 4. EL spectra of the phosphor-free white LED and the as-grown. Insets show photographs of the packaged devices operated at 20 mA and 1 mA respectively.

while the as-grown LED has an emission peak centered at around 608 nm – 642 nm.The centre wavelengths are voltage dependent due to band filling effects. The blue peak can be attributed to emission from individual nanopillars and small nano-clusters which exhibit large spectral blue-shifts due to strain relaxation. As the band filling effect is less pronounced for the strain-relaxed nanopillars and smaller nano-clusters, their emission converge to form the blue spectral peak with increasing currents. The green/yellow peak has a broader spectral width which can be attributed to a mixture of emission from the diverse range of sizes of nano-islands due to clustering. As a larger ratio of surface area is exposed, the wet etch has a more pronounced effect on individual nanopillars than on the nano-islands. As shown in Fig. 3(f), the diameters of the individual nanopillars are reduced to around 50 nm after the wet etch, while the sizes of the nano-islands are less affected, opening up a gap in size distribution and thus the two prominent spectral peaks. Fig. 3(g) is microphotograph of the nanopillar LED operated at a bias voltage of 3.8V, showing emission at different colors from different regions of the emissive region mixing into white-light emission. μ-EL spectra collected at different locations of the emissive region using a lensed fiber (WT&T CL5) with a focus spot of 1 μm are shown in Fig. 3(i), illustrative of the emission wavelength variations across the device. The color characteristics of the device is demonstrated in the CIE color chromaticity diagram of Fig. 5(c), with the whitest point at the CIE coordinate of (0.30, 0.35) at a bias voltage of 3.94V. The phosphor-free nanopillar LED achieves a Color Rendering Index (CRI) of around 76 and a overall luminous efficacy of 2.6 lm/W at a DC bias voltage of 3V (current of 6 mA); both parameters drop gradually with increasing voltage, owing to an increase in intensity of the blue spectral peak due to band filling effect.

The performance of the LED improves under pulsed operation as plotted in Fig. 5(a), suggesting that there is room for improvement with improved heat sinking. A maximum overall luminous efficacy of 11.0 lm/W can be achieved when the LED is driven with 600 ns 3V pulses at a frequency of 150 kHz. As shown in Fig. 5(b), the optical output power of the nanopillar LED is ~31.8% of the as-grown LED at a voltage of 3V; given that the summed area of the nanopillars is 32.4% of the as-grown, their areal power densities are on-par with each other. As the voltage increases, the gap in optical power narrows down to about 61.8% at a bias voltage of 4.5V, suggesting that the nanopillar LED experiences less droop effects[16].

The performance of this phosphor-free white LED is on par with the device reported in Ref. 3, which demonstrated an overall luminous efficacy of 7.92 lm/W and a CRI of 80 under DC operation. It is envisaged that the performance of the device can be further improved with increasing IQEs of long wavelength-emitting wafers[17]. The performance can also benefit from increased packing densities of nanopillars to retain most of the active region; this may be accomplished by replacing the silica nanospheres with metallic nanospheres which have higher etch selectivity, so that nanospheres with smaller dimensions can be used.

In summary, a phosphor-free white-light LED fabricated by nanosphere lithography with mono-sized nanospheres is

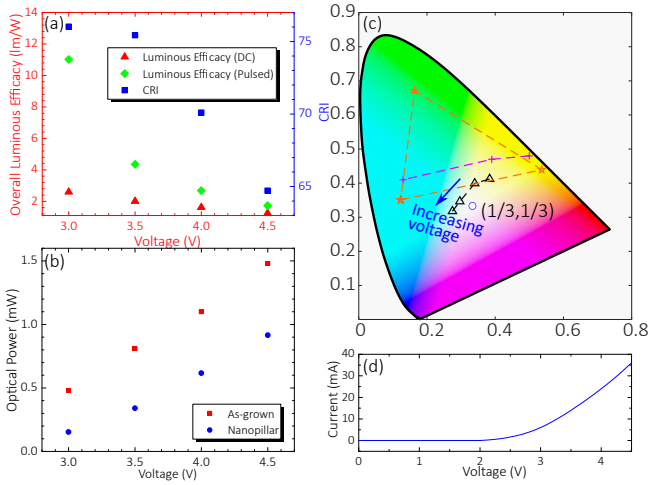

FIG. 5. (a) CRI and overall luminous efficacy of phosphor-free white-light LED at different bias voltages measured under DC and pulsed operations, (b) Optical output powers of phosphor-free white-light LED and the as-grown LED with respect to bias DC voltages, and (c) CIE chromaticity diagrams plotting the CIE coordinates of the phosphor-free white-light LED under different operating conditions. The black line with triangular markers corresponds to the data in this work, while the purple and orange lines correspond to data from previous studies by Feng *et al.*[8] and Chung *et al.*[13], respectively. (d) shows the IV curve of the device.

demonstrated in this work. The extent of spectral shift experienced by the InGaN/GaN quantum wells depends on the nanopillar diameter as determined by molecular dynamics simulations and $\mathbf{k}\cdot\mathbf{p}$ Schrödinger calculations. The nanosphere clustering pattern is designed with the aid of Monte Carlo simulations for achieving white-light emission from the nano-pillar LED. Phosphor-free white-light emission from the nano-pillar LED is demonstrated with a CRI of up to 76 and an overall luminous efficacy of 2.6 lm/W and 11.0 lm/W under DC and pulsed operations respectively.

This work was supported by the General Research Funds of the Research Grant Council of Hong Kong (17204218 & 17205318). The computations were performed using research computing facilities offered by HKU Information Technology Services.

DATA AVAILABILITY

The data that supports the findings of this study are available within the article.

REFERENCES

[1] K. H. Li, W. Y. Fu, and H. W. Choi, "Chip-scale gan integration," Progress in Quantum Electronics **70**, 100247 (2020).

[2] B. Damilano, N. Grandjean, C. Pernot, and J. Massies, "Monolithic white light emitting diodes based on ingan/gan multiple-quantum wells," Japanese Journal of Applied Physics Part 2-Letters **40**, L918–L920 (2001).

[3]M. Yamada, Y. Narukawa, and T. Mukai, "Phosphor free high-luminous-efficiency white light-emitting diodes composed of ingan multi-quantum well," Japanese Journal of Applied Physics **41**, L246–L248 (2002).

[4]D. Iida, Z. Zhuang, P. Kirilenko, M. Velazquez-Rizo, and K. Ohkawa, "High-color-rendering-index phosphor-free ingan-based white light-emitting diodes by carrier injection enhancement via v-pits," Applied Physics Letters **117**, 172103 (2020).

[5]B. Damilano, A. Dussaigne, J. Brault, T. Huault, F. Natali, P. Demolon, P. D. Mierry, S. Chenot, and J. Massies, "Monolithic white light emitting diodes using a (ga,in)n/gan multiple quantum well light converter," Applied Physics Letters **93**, 101117 (2008).

[6]S. J. Chua, C. B. Soh, W. Liu, J. H. Teng, S. S. Ang, and S. L. Teo, "Quantum dots excited ingan/gan phosphor-free white leds," physica status solidi c **5**, 2189–2191 (2008).

[7]K. Kishino, N. Sakakibara, K. Narita, and T. Oto, "Two-dimensional multicolor (rgby) integrated nanocolumn micro-leds as a fundamental technology of micro-led display," Applied Physics Express **13**, 014003 (2019).

[8]C. Feng, J.-A. Huang, and H. W. Choi, "Monolithic broadband ingan light-emitting diode," ACS Photonics **3**, 1294–1300 (2016).

[9]R. Debnath, J.-Y. Ha, B. Wen, D. Paramanik, A. Motayed, M. R. King, and A. V. Davydov, "Top-down fabrication of large-area gan micro- and nanopillars," Journal of Vacuum Science & Technology B **32**, 021204 (2014).

[10]Q. Wang, J. Bai, Y. P. Gong, and T. Wang, "Influence of strain relaxation on the optical properties of ingan/gan multiple quantum well nanorods," Journal of Physics D-Applied Physics **44**, 395102 (2011).

[11]Y. R. Wu, C. H. Chiu, C. Y. Chang, P. C. Yu, and H. C. Kuo, "Size-dependent strain relaxation and optical characteristics of ingan/gan nanorod leds," IEEE Journal of Selected Topics in Quantum Electronics **15**, 1226–1233 (2009).

[12]H. W. Choi, "White nanoled without requiring color conversion," (US Patent 9,401,453, 2013).

[13]K. Chung, J. Sui, B. Demory, and P.-C. Ku, "Color mixing from monolithically integrated ingan-based light-emitting diodes by local strain engineering," Applied Physics Letters **111**, 041101 (2017).

[14]W. Y. Fu and H. W. Choi, "Explaining relative spectral red-shifts in ingan/gan micropillars," Optica **5**, 765–773 (2018).

[15]W. Y. Fu and H. W. Choi, "Strain-induced spectral red-shifting from nanoscale frustum arrays fabricated over ingan/gan quantum wells for light-emitting applications," ACS Applied Nano Materials **4**, 666–672 (2021).

[16]Z. Gong, B. Guilhabert, Z. Chen, and M. D. Dawson, "Direct led writing of submicron resist patterns: Towards the fabrication of individually-addressable ingan submicron stripe-shaped led arrays," Nano Research **7**, 1849–1860 (2014).

[17]A. Dussaigne, F. Barbier, B. Samuel, A. Even, R. Templier, F. Lévy, O. Ledoux, M. Rozhavskaia, and D. Sotta, "Strongly reduced v pit density on inganos substrate by using ingan/gan superlattice," Journal of Crystal Growth **533**, 125481 (2020).